How to cite: *Angew. Chem. Int. Ed.* **2024**, *63*, e202320008
doi.org/10.1002/anie.202320008

Alkane Separation

A Microporous Multi-Cage Metal–Organic Framework for an Effective One-Step Separation of Branched Alkanes Feeds

Lin Zhou[+], Pedro Brântuas[+], Adriano Henrique[+], Helge Reinsch[+], Mohammad Wahiduzzaman[+], Jean-Marc Grenèche, Alírio E. Rodrigues, José A. C. Silva, Guillaume Maurin,* and Christian Serre**

[*] L. Zhou,[+] C. Serre
Institut des Matériaux Poreux de Paris, ESPCI Paris, Ecole Normale Supérieure, CNRS, PSL University, 75005, Paris, France
E-mail: christian.serre@espci.psl.eu

L. Zhou[+]
Key Laboratory of Biomass Chemical Engineering of Ministry of Education, College of Chemical and Biological Engineering, Zhejiang University, 310027, Hangzhou, China

L. Zhou[+]
Institute of Applied Micro-Nano Materials, School of Physical Science and Engineering, Beijing Jiaotong University, 100044, Beijing, China

L. Zhou[+]
Zhejiang Baima Lake Laboratory Co., Ltd., 310052, Hangzhou,-China

P. Brântuas,[+] A. Henrique,[+] J. A. C. Silva
Centro de Investigação de Montanha (CIMO), Instituto Politécnico de Bragança, Campus de Santa Apolónia, 5300-253 Bragança, Portugal
E-mail: jsilva@ipb.pt

P. Brântuas,[+] A. Henrique,[+] J. A. C. Silva
Laboratório Associado para a Sustentabilidade e Tecnologia em Regiões de Montanha (LA SusTEC), Instituto Politécnico de Bragança, Campus de Santa Apolónia, 5300-253 Bragança, Portugal

A. Henrique,[+] A. E. Rodrigues
Laboratory of Separation and Reaction Engineering (LSRE), Associate Laboratory LSRE/LCM, Department of Chemical Engineering, Faculty of Engineering University of Porto, Rua Dr. Roberto Frias, S/N, 4200-465 Porto, Portugal

A. Henrique,[+] A. E. Rodrigues
Associate Laboratory in Chemical Engineering (ALiCE), Faculdade de Engenharia, Universidade do Porto, R. Dr. Roberto Frias, S/N, 4200-465, Porto, Portugal

H. Reinsch[+]
Department for Inorganic Chemistry, University of Kiel, Max-Eyth Straße 2, 24118 Kiel, Germany

M. Wahiduzzaman,[+] G. Maurin
ICGM, Univ. Montpellier, CNRS, ENSCM 34293 Montpellier, France
E-mail: guilaume.maurin1@umontpellier.fr

J.-M. Grenèche
Institut des Molécules et Matériaux du Mans (IMMM), UMR 6283 CNRS, Le Mans Université, 72085 Le Mans Cedex 9, France

[+] These authors contributed equally to this work.

Abstract: The improvement of the Total Isomerization Process (TIP) for the production of high-quality gasoline with the ultimate goal of reaching a Research Octane Number (RON) higher than 92 requires the use of specific sorbents to separate pentane and hexane isomers into classes of linear, mono- and di-branched isomers. Herein we report the design of a new multi-cage microporous Fe(III)-MOF (referred to as MIP-214, MIP stands for materials of the Institute of Porous Materials of Paris) with a **flu-e** topology, incorporating an asymmetric heterofunctional ditopic ligand, 4-pyrazolecarboxylic acid, that exhibits an appropriate microporous structure for a thermodynamic-controlled separation of hydrocarbon isomers. This MOF produced via a direct, scalable, and mild synthesis route was proven to encompass a unique separation of C5/C6 isomers by classes of low RON over high RON alkanes with a sorption hierarchy: (n-hexane $\gg$ n-pentane $\approx$ 2-methylpentane $>$ 3-methylpentane)$_{low\ RON}$ $\gg$ (2,3-dimethylbutane $\approx$ i-pentane $\approx$ 2,2-dimethylbutane)$_{high\ RON}$ following the adsorption enthalpy sequence. We reveal for the first time that a single sorbent can efficiently separate such a complex mixture of high RON di-branched hexane and mono-branched pentane isomers from their low RON counterparts, which is a major achievement reported so far.

Purifying hydrocarbons with advanced separation processes (e.g. adsorption, membranes, etc.) is crucial in petrochemical industry due to the high energy penalty of the conventional separation processes of chemical mixtures (e.g. distillation).[1] In the manufacture of gasoline, its quality is measured by the research octane number (RON) above 90, fundamental for the efficient combustion of thermal engines. A high research octane number (high RON—HRON) in gasoline blends is closely related to the level of branched pentane (C5) and hexane (C6) alkane molecules. With the advent of manufacturing unleaded gasoline, cracking, alkylation, isomerization, and the use of additives are strategies to increase the RON of gasoline to above 92. Regarding the isomerization processes, e.g., the Total Isomerization Process (TIP) from Universal Oil Products (UOP)[2–4] and the analog Ipsorb/Hexorb process from Axens,[5–7] the catalytic reaction where the linear alkanes (low RON—LRON;

present in large amount in light naphtha) are isomerized to branched alkanes is followed by a separation step in which an adsorbent is used to completely separate the branched alkanes from the unconverted linear alkanes. The output of the isomerization reactor and the respective feed to the adsorption separation unit are mainly composed of di-branched alkanes: 2,2-dimethylbutane (22DMB; RON 94) and 2,3-dimethylbutane (23DMB; RON 105), mono-branched alkanes: 2-methylpentane (2MP; RON 74.4), 3-methylpentane (3MP; RON 75.5) and i-pentane (iC5; RON 93.5), and linear alkanes: n-hexane (nC6; RON 30) and n-pentane (nC5; RON 61.7).[2] The adsorption separation unit in actual TIP processes uses zeolite 5A (LTA type) with 8-ring apertures, which only separates the linear isomers (nC5 and nC6) from the branched ones (22DMB, 23DMB, 2MP, 3MP, and iC5), returning them back to the isomerization reactor for further processing, while the other isomers are removed as the final product. However, the presence of a large amount of LRON mono-branched C6 isomers, 2MP and 3MP (ca. 30 %), is detrimental to the octane upgrading of gasoline for RON values higher than 90. Therefore, it is of great importance to develop new advanced adsorbents to replace zeolite 5A and efficiently separate the high HRON isomers (22DMB, 23DMB, and iC5) from the other LRON alkanes to achieve upgraded gasoline blends (RON > 90) without using additives that usually significantly increase the final product price.

The separation of C6 isomers by zeolites or metal–organic frameworks (MOFs) with various topologies has been intensively investigated.[8–14] Among the zeolites that are adequate for the splitting of LRON/HRON branched alkanes, MFI (with 10-ring channels) and BEA (with 12-ring channels) types (with larger pore openings than LTA) can discriminate fractions with HRON content. However, this is achieved via a slow kinetic diffusion mechanism (MFI) or a low thermodynamic selectivity (BEA).[15–18] Porous MOFs due to their pore shape/size that can be systematically varied by the judicious choice of metal ions, bridging organic linkers, and structure types are a suitable alternative for such separation.[19–21] The features of MOFs as practical adsorbents are quite different from zeolites, whose pores are confined by rigid tetrahedral oxide skeletons with limited chemical variability. Specifically, the microporous MOFs with suitable pore aperture sizes and/or pore shapes have shown great potential for separating C6 isomers by classes of HRON/LRON. For instance, a kinetic separation can be achieved between the HRON 22DMB and the LRON isomers 3MP and nC6 with MIL-53(Fe)-$(CF_3)_2$.[22] Via a thermodynamic equilibrium selectivity, $Fe_2(BDP)_3$ and MIL-140B both with 1D triangular channels (that are unattainable in zeolites) were found to conveniently separate linear, mono and di-branched alkane molecules.[23,24] Also, a further precise construction of the Zr-abtc and CAU-10-H/Br MOFs with square-shaped channels allows discriminating the same mixture via a thermodynamic and kinetic mechanisms, respectively.[25,26] Remarkably, HIAM-203 and Ca-(H_2tcpb) (two calcium-based materials) have the ability to molecular sieve 22DMB from 3MP and nC6, based on a temperature programming separation process due to their structure flexibility.[11,27] Similar outcomes were also shown by MOF adsorbents possessing a robust framework with optimal pore channels, such as Zn-tcpt, Al-bttotb and NU-2004.[12,28,29] However, most of these studies with MOFs are currently being performed with only C6 alkane isomers and not all show multicomponent data.[29]

In the case of the more complex C5 and C6 alkane mixtures representative of light naphtha, an effective discrimination of the three desirable HRON compounds (22DMB, 23DMB, and iC5) from the four LRON isomers (2MP, 3MP, nC6, and nC5) for improving the overall RON of the final product of TIP processes is highly challenging. With respect to both C5 and C6 alkane mixtures, configurational bias Monte Carlo (CBMC) simulations predicted for the 1D channels of the benchmark MOF $Fe_2(BDP)_3$ a poor discrimination of the HRON C5 isomer iC5 relative to the LRON mono-branched C6 isomers 2MP and 3MP, which is detrimental for overall performance of the TIP process.[23] Very recently, some of us have shown that such a complete separation between C5 and C6 HRON and LRON isomers can be performed through a synergistic action of two families of sorbent materials: (i) the microporous bioderived MOF, MIL-160(Al), that thermodynamically separates C6 isomers according to the degree of branching, and (ii) the commercial zeolite 5A that molecular sieve rejects branched isomers, leading to an unprecedented final product RON of 92.[30] However, so far, none of the existing porous adsorbents including zeolites and MOFs enable to achieve this highly challenging separation through a single adsorbent. Therefore, we ambition here to develop a new MOF with the unique ability to perform a single one-step separation. This major achievement eliminates the need to use mixed or layered beds in cyclic industrial operations (MIL-160(Al)/zeolite 5A). Accordingly, Figure 1 illustrates the concept aiming to develop the new MOF MIP-214 (MIP stands for materials of the Institute of Porous Materials of Paris).

To reach such an ambitious objective, we deployed an isoreticular chemistry approach, by substituting one ligand by another one with a similar geometry/complexing group and a different size/length. For the target C5/C6 alkanes separation, the desired MOFs shall exhibit narrow pores. Thus, we opted to substitute long-length ligands from existing large-pore MOFs with shorter ligands. Typically, the replacement of linear terephthalic acid linker (6.9 Å in length) by shorter fumaric acid (5.0 Å in length) in MOF-5, MIL-53, and UiO-66 type architectures resulted in contracted versions of these materials, some of them exhibiting excellent performance for hydrocarbon separations, however still not meeting the ideal performances, either in terms of selectivity or productivity.[31–34] Thus, we envision that designing a MOF with narrow pore apertures and a very large internal pore volume would be highly desirable for optimal separation of branched alkanes since their constricted apertures would improve the adsorptive selectivity while the cage-like pores would lead to a higher sorption capacity. Such a strategy has already been applied to design MOFs with enhanced separation ability, including alkane isomers separation.[12,25,35,36] When considering structures

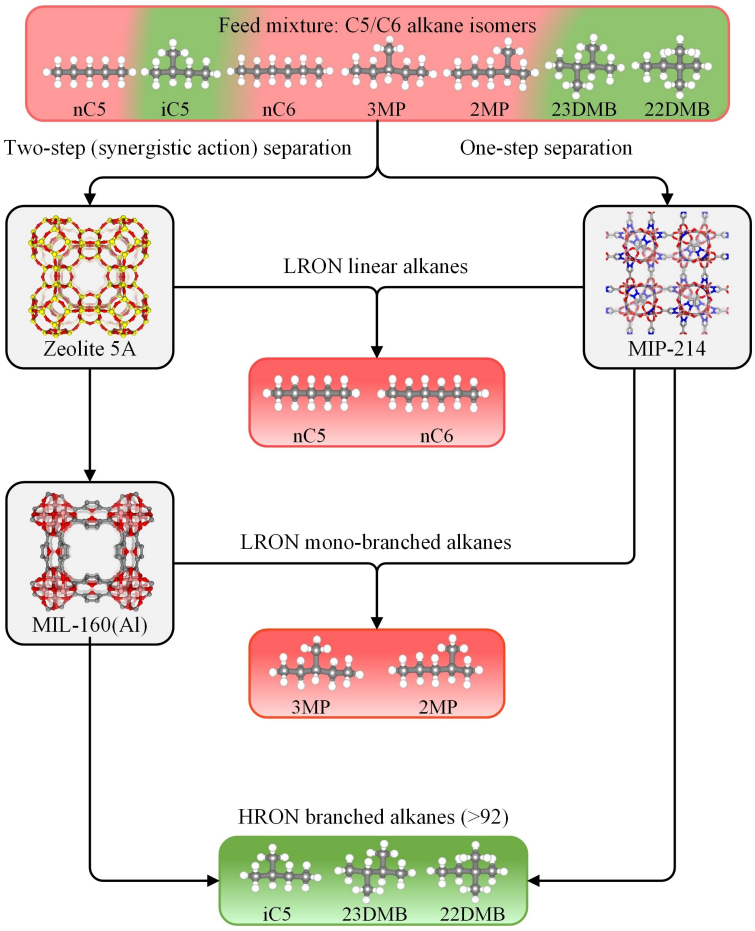

Figure 1. Schematic illustration of the separation of C5/C6 alkane isomers into fractions of LRON and HRON alkanes via: Left—Two-step (synergistic action) separation with zeolite 5A and MIL-160(Al).[30] Right: One-step separation using MIP-214.

with such a configuration, the MTN zeotype architecture MOFs emerge as attractive candidates—such as the benchmark mesoporous MOFs: MIL-100[37] and MIL-101.[38] However, these MOFs possess large microporous windows, far too big for a size exclusion-based separation of alkanes. A contracted version of MIL-101 with MTN topology, or of the hypothetical MIL-hypo-2,[39] predicted a few decades ago, was recently reported as MCF-48.[40] It exhibits **flu-e** topology with large multi-cages accessible through smaller square-shaped windows, likely to exhibit a higher shape/size-based adsorption selectivity compared to the larger pentagonal (φ~12,5 Å) and hexagonal (φ~16 Å) windows of MIL-101 metal(III) terephthalate mesoporous materials. Its microporous apertures, however, still slightly exceed the size required to separate branched alkanes. Herein, with the aim to construct a multi-cage MOF to potentially achieve a highly efficient pentane/hexane isomers separation into classes of HRON and LRON counterparts, we deliberately designed a new microporous Fe(III) trimer-based MOF MIP-214, of formula $[Fe_3(OH)(H_2O)_2(\mu_3\text{-}O)(PyC)_3]\cdot guest$ (*guest* = H_2O, DMF) by using an off-the-shelf small asymmetric heterofunctional ditopic ligand, 4-pyrazolecarboxylic acid (H_2PyC, 4.0 Å in length) to replace the terephthalic acid linker used in MCF-48 with **flu-e** topology (Figure 2), associated with microporous apertures (~6.1 Å) and large cages (~10.5 Å and 15 Å).

Simply through the reaction of $Fe(NO_3)_3\cdot 9H_2O$ and H_2PyC with a mole ratio of 1:1 in N,N′-dimethylformamide (DMF) under 353 K, yellowish green MIP-214 was isolated and further purified by DMF and methanol washing. Noteworthy, the synthesis is easily scalable up to ~25 g using similar ambient pressure conditions (Figures S1, S2). The crystal structure of MIP-214 was solved ab initio from high-resolution powder X-ray diffraction (PXRD) data (Figures S8, S9; Tables S2, S3). It indicates that the solid crystallizes in a cubic Fm-3 m space group (n° 225) with a unit-cell parameter of $a = 31.800(5)$ Å and $V = 31800(4)$ Å^3. The framework is constructed by the linkage of PyC^{2-} anions and inorganic Fe_3O trimers containing clusters that consist of three Fe atoms in an octahedral environment with one μ_3-O atom, four oxygen and/or nitrogen atoms from statistically disordered carboxylate groups and/or pyrazolate rings from four independent PyC^{2-} ligands and one oxygen atom from the terminal water. The Mossbauer spectra obtained at 300 K and 77 K are similar (only the 77 K spectrum is illustrated in Figure S6): they result exclusively from an asymmetrical quadrupolar doublet with broadened lines. It is important to note a great similarity with the MOF sample

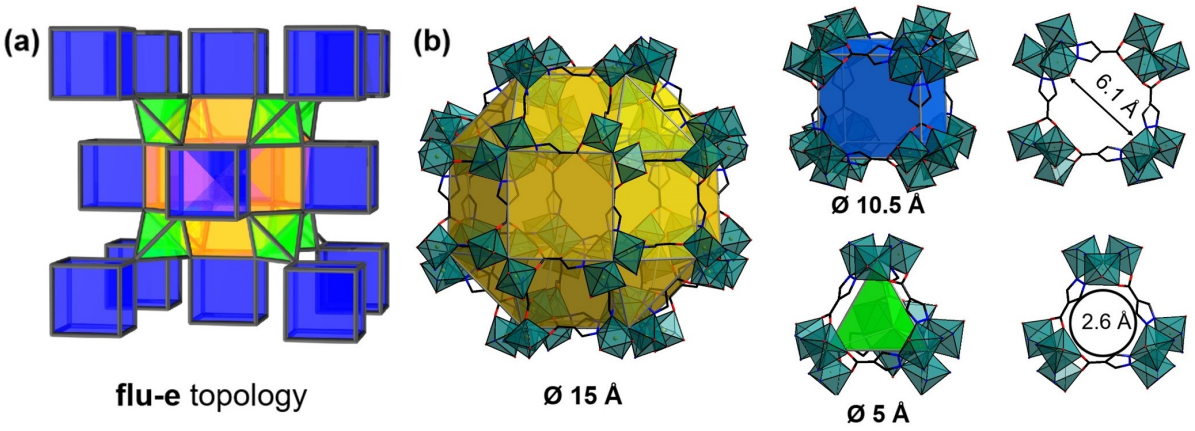

Figure 2. (a) The **flu-e** net of MIP-214 structure. (b) The rhombicuboctahedron, cube, and tetrahedron cages, as well as the shared square and triangular windows of MIP-214. Fe polyhedra, carbon atoms, nitrogen atoms and oxygen atoms are in bluish green, black blue and red, respectively. Hydrogen atoms have been omitted for clarity.

MIL-100(Fe): indeed, these samples contain the same Fe_3O trimers although in our case (MIP-214), the real environment is FeX_6 (X=O, N) versus FeO_6 for MIL-100(Fe). The best fitting model requires at least two quadrupolar components, but a model involving three quadrupolar components is physically more realistic. The refined values of the hyperfine parameters are listed in Table S1. The isomer shift values, which are also very similar, indicate unambiguously the presence of Fe^{3+} species located in FeX_6 octahedral units (X=O, N). The lack of resolution leads to a variety of solutions, but the hyperfine structures suggest three rather equiprobable iron sites with different chemical environments, which agrees quite well with the crystallographic structure as described above.

Notably, these trinuclear clusters based on mixed carboxylates and pyrazolates are unprecedented. The pyrazole bears a negative charge, and the two nitrogen atoms from the pyrazole bind in a similar way as a carbxylate with the iron trimer of octahedra. An attempt to remove the disorder of the carboxylate/pyrazolate groups reduces the space group to P213 or P23. These statistically equivalent systems were further geometry optimized at the density-functional level of theory (DFT). The simulated PXRD patterns of these DFT derived models show excellent similarities with the experimental one (Figure S2), further confirming the accuracy of the ab initio determined model of MIP-214.

Further structural analysis revealed that MIP-214 exhibits the same **flu-e** topology (Figure 2a) as chromium terephthalate-based MIL-hypo-2 structure predicted previously[39] and its Fe-analogue MCF-48 synthesized following a rather complex stepwise process.[40] Remarkably, MIP-214 is a contracted version of MCF-48, which can be realized in more direct and mild synthesis conditions. In the **flu-e** net of the MIP-214, the Fe trimer-based clusters act as the vertex, and the PyC^{2-} anions act as the edges. Small tetrahedra (diameter of ~5 Å), medium cubes (diameter of ~10.5 Å), and large rhombicuboctahedra (diameter of ~15 Å) with a ratio of 2:1:1 are formed by sharing the inorganic trimer clusters and/or the square (~6.2 Å) and triangle (~2.6 Å) windows. For the sake of clarity, consistent with the DFT optimized models, we show the framework cages and windows without any disorder in Figures 2b, S10. The reversible type-I N_2-sorption isotherm (Figure S7) leads to a BET area of 1140 $m^2 g^{-1}$ and a pore volume of 0.46 $cm^3 g^{-1}$, much higher than those of zeolite 5A (~600 $m^2 g^{-1}$ and 0.25 $cm^3 g^{-1}$, respectively).[25] A slight deviation between the experimetal and theoretical surface area and pore volume (1650 $m^2 g^{-1}$ and 0.56 $cm^3 g^{-1}$) values was observed, as is often the case with MOF materials that are not easy porous solids to activate, unlike zeolites that can be cleaned through calcination. The pore size distribution (PSD) and associated pore network of the MIP-214 are presented in Figure S23: a good agreement is found between the theoretical values and the calculated PSD deduced from experimental data using the NLDFT model. TGA curve (Figure S5) indicates the complete departure of organic ligands at around 490 K in oxygen. Interestingly, MIP-214 exposed to air maintains its crystallinity over 1.5 years (see the PXRD patterns in Figure S2), likely due to the strong Fe(III) carboxylate bonds, while Fe-pyrazolates are usually more prone to hydrolysis.

The alkane isomers separation performance of MIP-214 was assessed using a chromatographic technique through dynamic breakthrough experiments (Figure S13).[41] The separation of a quinary mixture of equimolar C6 isomers was first investigated, followed by the separation of a septenary mixture of equimolar C5/C6 isomers. These experimental studies were carried out at 343 K and 373 K and at 10, 25, and 50 kPa of total isomers pressure (Tables S5, S6).

The breakthrough experiment with C6 isomers is shown in Figure 3a at 373 K and a total isomers pressure of 10 kPa, where it is noted that all isomers are able to diffuse through the square windows of MIP-214. Note that window sizes smaller than or comparable to those of the guests do not necessarily mean a diffusion problem and/or kinetic separation mechanism owing to the flexible nature of the apertures

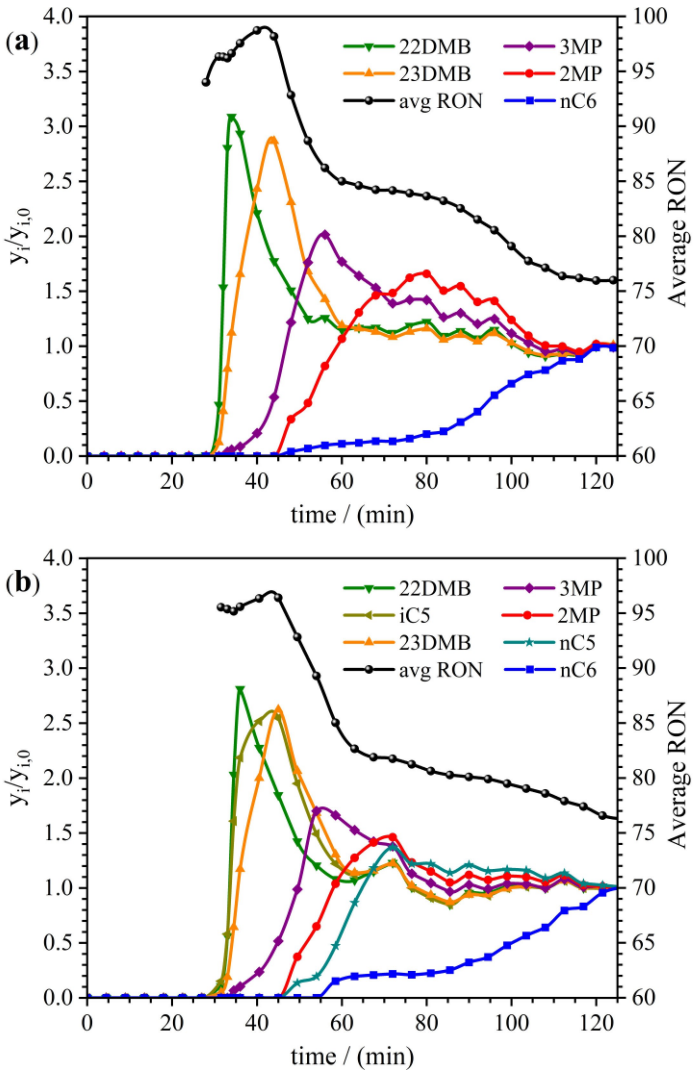

Figure 3. Separation of equimolar mixtures of C6 isomers (a) and C5 and C6 isomers (b) by fixed bed adsorption with MIP-214 at 373 K and a total isomers pressure of 10 kPa. Breakthrough data is plotted as the normalized molar fraction of each isomer (left y-axis) and average real-time RON (right y-axis) as a function of time.

and/or the guest molecules.[42] Notably, we remark that the di-branched isomers 22DMB followed by 23DMB elute first from the column, then the mono-branched isomers 3MP followed by 2MP eluted subsequently, and lastly, the nC6. Indeed, MIP-214 enables a separation according to the degree of branching: linear (nC6) ⩾ mono-branched (2MP, 3MP) ⩾ di-branched (22DMB, 23DMB). This separation sequence depicted in Figure 3a is similar for most materials with channel-like pores mentioned above. Decisively, MIP-214 can even separate the two mono-branched isomers (2MP and 3MP) of similar kinetic diameter (5 Å), which are unlikely to be realized by other benchmark materials, $Fe_2(BDP)_3$ or Al-bttotb with 1D channels.[23,28] This demonstrates the finely shape-based discrimination of hexane isomers through the cage-like structure of MIP-214. The two most desirable di-branched isomers with HRON values show an overshoot up to more than two or even three times the initial feed concentrations due to the competitive adsorption equilibrium between different isomers. The observed adsorption hierarchy nC6 ⩾ 2MP > 3MP > 23DMB ≈ 22DMB is kept in the full range of investigated pressures and temperatures: 343 K to 373 K and partial pressure up to 50 kPa (Figures S14, S15). The measured adsorption selectivity calculated by Eq. S4 from the breakthrough data increases from 4.5 (343 K, 50 kPa—Figure S14c) to 21.2 (373 K, 10 kPa—Figure 3a). MIP-214 also falls within the best performing MOFs (selectivity > 10 and adsorption capacity > 0.6 mol kg^{-1}) predicted by two recent high-throughput computational studies.[43,44] Of relevance to the industrial processes, MIP-214 has significantly high ideal productivities (> 0.74 mol dm^{-3}, Table S5) for a fixed RON of 92, outperforming the majority of current adsorbent materials (see Table S7), including the benchmark $Fe_2(BDP)_3$ MOF (0.54 mol dm^{-3}) by at least 40 %.[23]

CBMC adsorption simulations were then performed for the equimolar quinary mixture of C6 isomers at 373 K. They

evidenced the same hierarchy as that observed experimentally by breakthrough experiments: nC6 ≫ 2MP > 3MP > 23DMB ≈ 22DMB (Figure 4a), following the sequence of adsorption enthalpies (Table S11, Figures 3a, S15). This conclusion remains also true at 343 K (Figures S14, S24a). A careful analysis of the CBMC-derived adsorption snapshots revealed more favorable adsorption of nC6 as compared to the other isomers in both cubic and rhombicuboctahedron cages (Figures 5a and 5b). In addition, a significant fraction of the nC6 molecules sits perpendicularly in the gates/windows along the pathway connecting rhombicuboctahedral cages (Figures 5c, S22). The substantially higher uptake of nC6 is attributed to a much more efficient packing of this linear molecule over the entire porosity of MIP-214. The radial distribution functions (RDFs) calculated for the hydrocarbon/MOF atom pairs show that the shortest host/guest separating distances for all C6 isomers are ~3.6 Å, characteristic of relatively weak van der Waals interactions (Figure S25). The thermodynamic selectivity value, $S = 10.6$, calculated from the GCMC adsorption isotherms at 343 K for linear and mono-branched alkanes over di-branched ones at 10 kPa, was found to be similar to that determined from experimental breakthrough measurements (14.9). This value decreased to 6.3 (or 4.5 in the experimental data) at 50 kPa. Similar trends in adsorption selectivity were also observed at 373 K (Table S5).

Furthermore, for an equimolar mixture of all seven C5/C6 isomers, the breakthrough times of the C6 isomers follow the same sequence as in the separation of the quinary mixture (Figures 3b, S17, S18). Remarkably, with an adsorption hierarchy of nC6 ≫ nC5 ≈ 2MP > 3MP > 23DMB ≈ iC5 ≈ 22DMB, the high-octane di-branched 22DMB and 23DMB and mono-branched iC5 elute nearly together, much earlier than the elution of the other four LRON components, leading to an ideal 92 RON productivity of 0.67 mol dm^{-3} (comparable with the one calculated from the

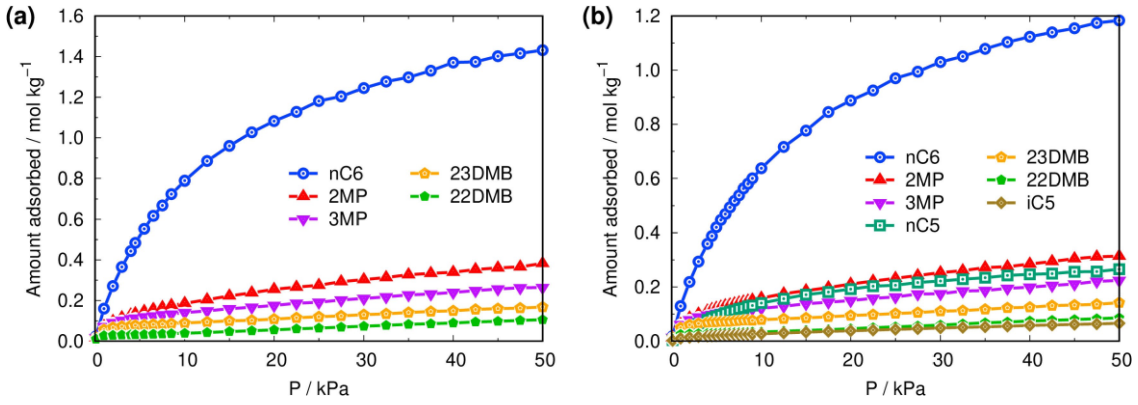

Figure 4. CBMC simulated adsorption isotherms of an equimolar quinary mixture of C6 isomers (a) and an equimolar septenary mixture of C5/C6 isomers (b) obtained for MIP-214 at 373 K.

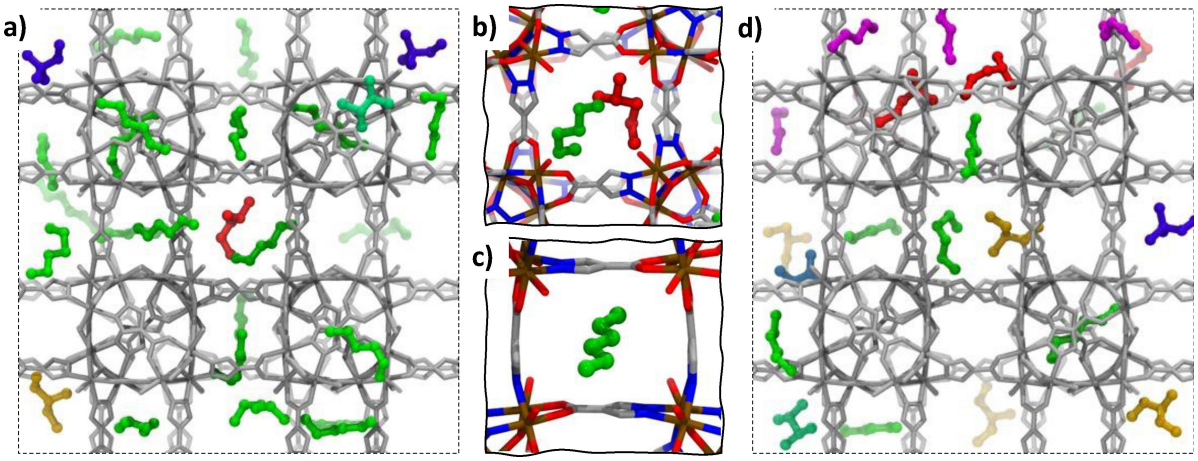

Figure 5. Illustration of the preferential arrangement of the adsorbed C6 and C5/C6 isomers in MIP-214 issued from the CBMC simulations performed for the equimolar quinary (a) and septenary mixtures (d), respectively, at $P = 10$ kPa and $T = 373$ K. Middle-panel shows magnified views of a nC6 molecule siting along the window of a rhombicuboctahedral cage (b), and a typical molecular packing (viz. nC6 along with a 2MP/3MP) inside a cubic cage (c). Color codes: nC6 (green spheres), 2MP (red spheres), 3MP (orange spheres), 23DMB (teal spheres) and 22DMB (violet spheres), nC5 (magenta spheres), and iC5 (light-blue spheres) and MIP-214 framework atoms are: Fe (dark orange), carbon (grey), nitrogen (blue), oxygen (red). MOF skeletons in a and d are depicted in mono-color grey, while hydrogen atoms are omitted for clarity.

experiment with only C6 isomers: 0.74 mol dm^{-3}) along with a selectivity of 11.3 (twice higher than that from the mixed-bed sorption of zeolite 5A and MIL-160(Al)[29]). This remarkable desired separation of HRON and LRON molecules is unique for all families of adsorbents, including zeolites and MOFs. Single-component adsorption equilibrium isotherms (Figure S21) derived from the single-component breakthrough curves of C5/C6 isomers in MIP-214 collected at 373 K (Figure S20) showed a similar sorption hierarchy order. The sharp breakthrough profiles prove that there are no kinetic limitations in the sorption of the C5/C6 isomers in MIP-214. Exceptionally, to the best of our knowledge, this is the first evidence of a single porous adsorbent being able to distinctly separate the HRON and LRON C5/C6 isomers in a one-step separation under practical operating conditions in the gas phase, which may decrease the complexity of the design of adsorption industrial processes by avoiding the use of mixed or layered beds.[30] CBMC simulations performed for the septenary C5/C6 mixture at 373 K and 343 K revealed the same adsorption sequence (Figures 4b, S24b). Similar to the equimolar quinary C6 mixtures, nC6 is adsorbed substantially more compared to the other alkanes in the mixture due to a favorable sitting in the cubic cages, as well as in the rhombicuboctahedron cages and their windows (Figure 5d). Here we noticed that linear nC5 molecules took over a few positions that would typically be occupied by nC6 ones, while these former molecules remain predominantly adsorbed as observed experimentally owing to a higher affinity of nC6 over nC5 (see Table S11). Overall, the adsorption enthalpy and Henry coefficient data calculated by MC widom insertion method indicate the strongest affinities of MIP-214 towards nC6 and nC5, followed by those of the monobranched C6 isomers and the weakest adsorption affinities towards dibranched C6 isomers and monobranched C5 isomer (the three most desired HRON components), revealing the thermodynamic separation mechanism. Indeed, this outstanding performance of MIP-214 showcases its exceptional potential in enhancing the TIP process, which can be attributed to its exceptional/unique ability to effectively separate HRON isomers, such as 22DMB, 23DMB, and iC5, from LRON isomers, specifically 3MP and 2MP.

In summary, a new microporous cubic MOF MIP-214 with **flu-e** topology, bearing narrow windows and large cages, was designed using a short ditopic ligand H_2PyC through an isoreticular chemistry approach. MIP-214 can be easily synthesized and scalable under mild conditions. The suitable pore structure (including small tetrahedron, medium cube, and large rhombicuboctahedron cages associated with square and triangle apertures) allows the diffusion of all C5 and C6 isomers, but with distinct affinities according to their shape and size. Breakthrough experiments revealed that this MOF enables a unique, effective one-step separation of the HRON and LRON alkane isomers fractions through a competitive thermodynamic adsorption process. MIP-214 is thus a promising candidate for HRON C5/C6 isomers class separation with the potential to be exploited in current TIP processes for the octane improvement of gasoline pools via a clean route, eliminating/reducing the need for additives in petrochemical industry.

Acknowledgements

L. Zhou acknowledges the support of the National Natural Science Foundation of China (22108246), "Pionner, Leading Goose + X" R&D Program of Zhejiang (2024SSYS0067) and the CSC scholarship (201707090054). Foundation for Science and Technology (FCT, Portugal) and ERDF under Programme PT2020 to: (1) Project ref: POCI01-0145-FEDER-016517 (PTDC/QEQ-PRS/3599/2014), (2) FCT/MCTES (PIDDAC) for financial support through national funds FCT/MCTES (PIDDAC) to CIMO (UIDB/00690/2020 and UIDP/00690/2020) and SusTEC (LA/P/0007/2020), (3) LSRE-LCM (POCI-01-0145-FEDER006984) and (4) Adriano Henrique from the individual research grant SFRH/BD/148525/2019. The simulation in this work was performed using HPC resources from GENCI-CINES (Grant A0140907613).

Conflict of Interest

The authors declare no conflict of interest.

Data Availability Statement

The data that support the findings of this study are available from the corresponding author upon reasonable request.

Keywords: Ultra-microporous metal–organic framework · Isoreticular Chemistry · Pentane and hexane alkane isomers separation · Octane upgrading of gasoline

[1] D. S. Sholl, R. P. Lively, *Nature* **2016**, *532(7600)*, 435–7, DOI: 10.1038/532435a.
[2] N. A. Cusher, In *Handbook of petroleum refining processes*; Meyers, R. A., Ed.; McGraw-Hill **2004**, pp 63–68.
[3] T. C. Holcombe, *n-Paraffin-isoparaffin separation process*, U.S. Patent, 4176053 **1979**.
[4] T. C. Holcombe, *Total isomerization process*, U.S. Patent, 4210771 **1980**.
[5] A. Minkkinen, L. Mank, S. Jullian, *Process for the isomerization of C5/C6 normal paraffins with recycling of normal paraffins*, U.S. Patent, 5233120 **1995**.
[6] B. Domergue, L. Watripont, *Petroleum technology quarterly* **2005**, *10(3)*, 21–25.
[7] S. Graeme, J. Ross, A. Nobel, N. Axens, In *Advanced solutions for paraffin isomerization*, Proceedings of the NPRA Annual Meeting, San Antonio, TX, March, **2004**, pp 21–23.
[8] H. Wang, J. Li, *Acc. Chem. Res.* **2019**, *52(7)*, 1968–1978, DOI: 10.1021/acs.accounts.8b00658.
[9] Z. Zhang, S. B. Peh, C. Kang, K. Chai, D. Zhao, *EnergyChem* **2021**, *3(4)*, DOI: 10.1016/j.enchem.2021.100057.
[10] L. Yu, S. Ullah, K. Zhou, Q. Xia, H. Wang, S. Tu, J. Huang, H.-L. Xia, X.-Y. Liu, T. Thonhauser, J. Li, *J. Am. Chem. Soc.* **2022**, *144*, 3766–3770. DOI: 10.1021/jacs.1c12068.

[11] Y. Lin, L. Yu, S. Ullah, X. Li, H. Wang, Q. Xia, T. Thonhauser, J. Li, *Angew. Chem. Int. Ed.* **2022**, *61*, e202214060. DOI: 10.1002/anie.202214060.
[12] L. Yu, S. Ullah, H. Wang, Q. Xia, T. Thonhauser, J. Li, *Angew. Chem. Int. Ed.* **2022**, *61*, e202211359. DOI: 10.1002/anie.202211359.
[13] F. Xie, L. Yu, H. Wang, J. Li, *Angew. Chem. Int. Ed.* **2023**, *62*, e202300722. DOI: 10.1002/anie.202300722.
[14] F.-A. Guo, J. Wang, C. Chen, X. Dong, X. Li, H. Wang, P. Guo, Y. Han, J. Li, *Angew. Chem. Int. Ed.* **2023**, *62*, e202303527. DOI: 10.1002/anie.202303527.
[15] A. F. P. Ferreira, M. C. Mittelmeijer-Hazeleger, A. Bliek, *Adsorption* **2007**, *13(2)*, 105–114, DOI: 10.1007/s10450-007-9010-z.
[16] A. F. P. Ferreira, M. C. Mittelmeijer-Hazeleger, J. v. d. Bergh, S. Aguado, J. C. Jansen, G. Rothenberg, A. E. Rodrigues, F. Kapteijn, *Microporous Mesoporous Mater.* **2013**, *170*, 26–35, DOI: 10.1016/j.micromeso.2012.11.020.
[17] P. S. Bárcia, J. A. C. Silva, A. E. Rodrigues, *Energy Fuels* **2010**, *24(3)*, 1931–1940, DOI: 10.1021/ef9013289.
[18] P. S. Barcia, J. A. C. Silva, A. E. Rodrigues, *Ind. Eng. Chem. Res.* **2006**, *45(12)*, 4316–4328, DOI: 10.1021/ie0513954.
[19] K. Adil, Y. Belmabkhout, R. S. Pillai, A. Cadiau, P. M. Bhatt, A. H. Assen, G. Maurin, M. Eddaoudi, *Chem. Soc. Rev.* **2017**, *46(11)*, 3402–3430, DOI: 10.1039/c7cs00153c.
[20] G. Maurin, C. Serre, A. Cooper, G. Férey, *Chem. Soc. Rev.* **2017**, *46(11)*, 3104–3107, DOI: 10.1039/c7cs90049j.
[21] L. Yang, S. Qian, X. Wang, X. Cui, B. Chen, H. Xing, *Chem. Soc. Rev.* **2020**, *49(15)*, 5359–5406, DOI: 10.1039/c9cs00756c.
[22] P. A. P. Mendes, P. Horcajada, S. Rives, H. Ren, A. E. Rodrigues, T. Devic, E. Magnier, P. Trens, H. Jobic, J. Ollivier, G. Maurin, C. Serre, J. A. C. Silva, *Adv. Funct. Mater.* **2014**, *24*, 7666–7673, DOI: 10.1002/adfm.201401974.
[23] Z. R. Herm, B. M. Wiers, J. A. Mason, J. M. van Baten, M. R. Hudson, P. Zajdel, C. M. Brown, N. Masciocchi, R. Krishna, J. R. Long, *Science* **2013**, *340(6135)*, 960–4, DOI: 10.1126/science.1234071.
[24] A. Henrique, T. Maity, H. L. Zhao, P. F. Brantuas, A. E. Rodrigues, F. Nouar, A. Ghoufi, G. Maurin, J. A. C. Silva, C. Serre, *J. Mater. Chem. A* **2020**, *8(34)*, 17780–17789, DOI: 10.1039/d0ta05538g.
[25] H. Wang, X. Dong, J. Lin, S. J. Teat, S. Jensen, J. Cure, E. V. Alexandrov, Q. Xia, K. Tan, Q. Wang, D. H. Olson, D. M. Proserpio, Y. J. Chabal, T. Thonhauser, J. Sun, Y. Han, J. Li, *Nat. Commun.* **2018**, *9(1)*, 1745, DOI: 10.1038/s41467-018-04152-5.
[26] Q. Yu, L. Guo, D. Lai, Z. Zhang, Q. Yang, Y. Yang, Q. Ren, Z. Bao, *Sep. Purif. Technol.* **2021**, *268*, 118646. DOI: 10.1016/j.seppur.2021.118646.
[27] H. Wang, X. Dong, E. Velasco, D. H. Oslon, Y. Han, J. Li, *Energy Environ. Sci.* **2018**, *11*, 1226–1231. DOI: 10.1039/C8EE00459E.
[28] L. Yu, X. Dong, Q. Gong, S. R. Acharya, Y. Lin, H. Wang, Y. Han, T. Thonhauser, J. Li, *J. Am. Chem. Soc.* **2020**, *142(15)*, 6925–6929, DOI: 10.1021/jacs.0c01769.
[29] K. B. Idrees, K. O. Kirlikovali, C. Setter, H. Xie, H. Brand, B. Lal, F. Sha, C. S. Smoljan, X. Wang, T. Islamoglu, L. K. Macreadie, O. K. Farha, *J. Am. Chem. Soc.* **2023**, DOI: 10.1021/jacs.3c04641.
[30] P. F. Brântuas, A. Henrique, M. Wahiduzzaman, A. Von Wedelstedt, T. Maity, A. Rodrigues, F. Nouar, U.-H. Lee, K. H. Cho, G. Maurin, J. A. C. Silva, C. Serre, *Adv. Sci.* **2022**, *9(22)*, 2201494, DOI: 10.1002/advs.202201494.
[31] E. Alvarez, N. Guillou, C. Martineau, B. Bueken, B. Van de Voorde, C. Le Guillouzer, P. Fabry, F. Nouar, F. Taulelle, D. de Vos, J. S. Chang, K. H. Cho, N. Ramsahye, T. Devic, M. Daturi, G. Maurin, C. Serre, *Angew. Chem. Int. Ed.* **2015**, *54(12)*, 3664–8, DOI: 10.1002/anie.201410459.
[32] A. H. Assen, Y. Belmabkhout, K. Adil, P. M. Bhatt, D. X. Xue, H. Jiang, M. Eddaoudi, *Angew. Chem. Int. Ed.* **2015**, *54(48)*, 14353–8, DOI: 10.1002/anie.201506345.
[33] M. Xue, Y. Liu, R. M. Schaffino, S. C. Xiang, X. J. Zhao, G. S. Zhu, S. L. Qiu, B. L. Chen, *Inorg. Chem.* **2009**, *48(11)*, 4649–4651, DOI: 10.1021/ic900486r.
[34] B. Bozbiyik, J. Lannoeye, D. E. De Vos, G. V. Baron, J. F. Denayer, *Phys. Chem. Chem. Phys.* **2016**, *18(4)*, 3294–301, DOI: 10.1039/c5cp06342f.
[35] H. Wang, X. Dong, V. Colombo, Q. Wang, Y. Liu, W. Liu, X.-L. Wang, X.-Y. Huang, D. M. Proserpio, A. Sironi, Y. Han, J. Li, *Adv. Mater.* **2018**, *30*, 1805088, DOI: 10.1002/adma.201805088.
[36] L. Yu, X. Han, H. Wang, S. Ullah, Q. Xia, W. Li, J. Li, I. Silva, P. Manuel, S. Rudić, Y. Cheng, S. Yang, T. Thonhauser, J. Li, *J. Am. Chem. Soc.* **2021**, *143*,19300–19305, DOI: 10.1021/jacs.1c10423.
[37] G. Férey, C. Serre, C. Mellot-Draznieks, F. Millange, S. Surblé, J. Dutour, I. Margiolaki, *Angew. Chem. Int. Ed.* **2004**, *116(46)*, 6456–6461, DOI: 10.1002/ange.200460592.
[38] G. Férey, C. Mellot-Draznieks, C. Serre, F. Millange, J. Dutour, S. Surble, I. Margiolaki, *Science* **2005**, *309(5743)*, 2040–2, DOI: 10.1126/science.1116275.
[39] C. Mellot-Draznieks, J. Dutour, G. Ferey, *Z. Anorg. Allg. Chem.* **2004**, *630(15)*, 2599–2604, DOI: 10.1002/zaac.200400416.
[40] J. Q. Shen, P. Q. Liao, D. D. Zhou, C. T. He, J. X. Wu, W. X. Zhang, J. P. Zhang, X. M. Chen, *J. Am. Chem. Soc.* **2017**, *139(5)*, 1778–1781, DOI: 10.1021/jacs.6b12353.
[41] A. Henrique, A. E. Rodrigues, J. A. C. Silva, *Sep. Purif. Technol.* **2020**, *238*, DOI: ARTN 116419 10.1016/j.seppur.2019.116419.
[42] D. Zhou, J. Zhang, *Acc. Chem. Res.* **2022**, *55(20)*, 2966–2977, DOI: 10.1021/acs.accounts.2c00418.
[43] Y. G. Chung, P. Bai, M. Haranczyk, K. T. Leperi, P. Li, H. D. Zhang, T. C. Wang, T. Duerinck, F. Q. You, J. T. Hupp, O. K. Farha, J. I. Siepmann, R. Q. Snurr, *Chem. Mater.* **2017**, *29(15)*, 6315–6328, DOI: 10.1021/acs.chemmater.7b01565.
[44] V. A. Solanki, B. Borah, *Ind. Eng. Chem. Res.* **2019**, *58(43)*, 20047–20065, DOI: 10.1021/acs.iecr.9b03533.

Manuscript received: December 27, 2023
Accepted manuscript online: February 15, 2024
Version of record online: March 4, 2024